

ACCEPTED VERSION

Tushar Kumeria, Htwe Mon, Moom Sinn Aw, Karan Gulati, Abel Santos, Hans J. Griesser, Dusan Losic

Advanced biopolymer-coated drug-releasing titania nanotubes (TNTs) implants with simultaneously enhanced osteoblast adhesion and antibacterial properties

Colloids and Surfaces B: Biointerfaces, 2015; 130:255-263

© 2015 Published by Elsevier B.V.

This manuscript version is made available under the CC-BY-NC-ND 4.0 license

<http://creativecommons.org/licenses/by-nc-nd/4.0/>

Final publication at <http://dx.doi.org/10.1016/j.colsurfb.2015.04.021>

PERMISSIONS

<http://www.elsevier.com/about/company-information/policies/sharing#acceptedmanuscript>

[Accepted manuscript](#)

Authors can share their accepted manuscript:

[...]

After the embargo period

- via non-commercial hosting platforms such as their institutional repository
- via commercial sites with which Elsevier has an agreement

In all cases accepted manuscripts should:

- link to the formal publication via its DOI
- bear a CC-BY-NC-ND license – this is easy to do, [click here](#) to find out how
- if aggregated with other manuscripts, for example in a repository or other site, be shared in alignment with our [hosting policy](#)
- not be added to or enhanced in any way to appear more like, or to substitute for, the published journal article

Embargo

0927-7765

Colloids and Surfaces B:
Biointerfaces

24

31 October 2017

<http://hdl.handle.net/2440/90952>

Accepted Manuscript

Title: Advanced biopolymer-coated drug-releasing titania nanotubes (TNTs) implants with simultaneously enhanced osteoblast adhesion and antibacterial properties

Author: Tushar Kumeria Htwe Mon Moom Sinn Aw Karan Gulati Abel Santos Hans J. Griesser Dusan Losic



PII: S0927-7765(15)00235-0
DOI: <http://dx.doi.org/doi:10.1016/j.colsurfb.2015.04.021>
Reference: COLSUB 7025

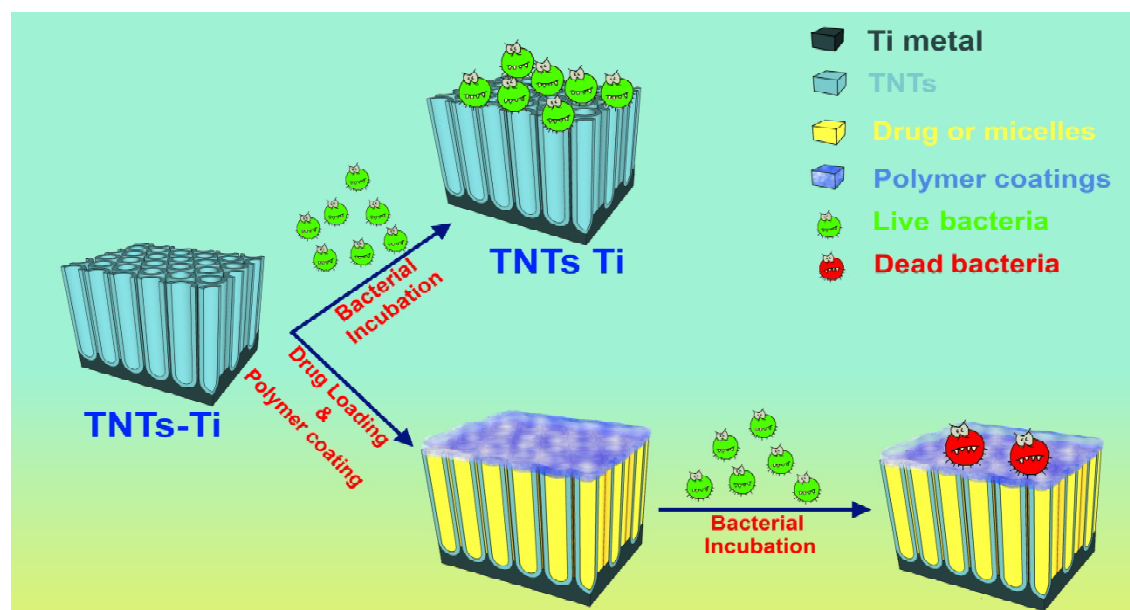
To appear in: *Colloids and Surfaces B: Biointerfaces*

Received date: 23-12-2014
Revised date: 25-3-2015
Accepted date: 8-4-2015

Please cite this article as: T. Kumeria, H. Mon, M.S. Aw, K. Gulati, A. Santos, H.J. Griesser, D. Losic, Advanced biopolymer-coated drug-releasing titania nanotubes (TNTs) implants with simultaneously enhanced osteoblast adhesion and antibacterial properties, *Colloids and Surfaces B: Biointerfaces* (2015), <http://dx.doi.org/10.1016/j.colsurfb.2015.04.021>

This is a PDF file of an unedited manuscript that has been accepted for publication. As a service to our customers we are providing this early version of the manuscript. The manuscript will undergo copyediting, typesetting, and review of the resulting proof before it is published in its final form. Please note that during the production process errors may be discovered which could affect the content, and all legal disclaimers that apply to the journal pertain.

GRAPHICAL ABSTRACT



Toward the development of titania nanotubes based multifunctional drug eluting Ti implants. The study presents a significant step development of multifunctional implants, able to simultaneously perform drug release, osteoblasts adhesion, and eradication of bacteria and biofilm. This study embarks on harnessing synergistic effects of the titania nanotubes (which act as container for drugs) and biopolymers (which have inherent antibacterial properties). Titania nanotubes (TNTs) grown on Ti implants are combined with biopolymer (Chitosan and PLGA) coatings to simultaneously enhance their antibacterial and osteogenic properties. Chitosan coated TNTs-Ti implants are able to effectively kill bacterial and promote osteoblast adhesion.

Highlights

- We fabricate TiO₂ nanotubes (TNTs) with controlled pore diameter and length on Ti substrate.
- Drug loading and release capabilities of these TNTs was explored using gentamicin as model drug. Drug release kinetics and burst release from TNTs was further controlled by biopolymer coating.
- Osteoblast adhesion activity suggested improved cell adhesion on TNTs surface than control surfaces (Ti plate or plastic surface). Osteoblast adhesion was greatest for biopolymer coated TNTs substrates (especially Chitosan).
- Antibacterial properties of gentamicin loaded TNTs suggest improved and long term antibacterial effect from biopolymer coated TNTs substrates.
- Chitosan coated TNTs displayed the best antibacterial and anti-biofilm formation capabilities.
- Altogether, biopolymer coated TNTs displayed simultaneous osteoblast adhesion and antibacterial properties.

Advanced biopolymer-coated drug-releasing titania nanotubes (TNTs) implants with simultaneously enhanced osteoblast adhesion and antibacterial properties

Tushar Kumeria^{1§}, Htwe Mon^{2§}, Moom Sinn Aw^{1§}, Karan Gulati¹, Abel Santos¹, Hans J. Griesser^{3}, Dusan Losic^{1*}*

¹School of Chemical Engineering, The University of Adelaide, Adelaide, SA 5005, Australia.

²Sansom Institute for Health Research, School of Pharmacy and Medical Sciences, University of South Australia, Frome Road, Adelaide SA 5000, Australia.

³Mawson Institute, Division of Information Technology, Engineering and the Environment, Building V, Mawson Lakes Campus, Mawson Lakes Boulevard, Mawson Lakes SA 5095, Australia.

Corresponding Author

Prof. Dusan Losic

School of Chemical Engineering, The University of Adelaide

Phone: +61 8 8313 1535 – Fax: +61 8 8303 4373

Email: dusan.losic@adelaide.edu.au ;

Prof. Hans J Griesser

Mawson Institute, Univeristy of South Australia

Phone: +61 8 830 23703– Fax: +61 8 830 25639

Email: hans.griesser@unisa.edu.au

[[§]] These authors contributed equally to this work.

KEYWORDS: Bone implants; Titania nanotubes; Drug release; Biopolymer coating; *Staphylococcus epidermidis*; Osteoblast cells..

ABSTRACT

Here, we report on the development of advanced biopolymer-coated drug-releasing implants based on titanium (Ti) featuring titania nanotubes (TNTs) on its surface. These TNTs arrays were fabricated on the Ti surface by electrochemical anodization, followed by the loading and release of a model antibiotic drug, gentamicin. The synergistic osteoblastic adhesion and antibacterial properties of these TNTs-Ti samples are significantly improved by loading antibacterial payloads inside the nanotubes and modifying their surface with two biopolymer coatings (PLGA and Chitosan). The improved osteoblast adhesion and antibacterial properties of these drug-releasing TNTs-Ti samples are confirmed by the adhesion and proliferation studies of osteoblasts and model gram-positive bacteria (*Staphylococcus epidermidis*). The adhesion of these cells on TNTs-Ti samples is monitored by fluorescence and scanning electron microscopies. Results reveal the ability of these biopolymer-coated drug-releasing TNTs-Ti substrates to promote osteoblasts adhesion and proliferation, while effectively preventing bacterial colonization by impeding their proliferation and biofilm formation. The proposed approach could overcome inherent problems associated with bacterial infections on Ti-based implants, simultaneously enabling the development of orthopedic implants with enhanced and synergistic antibacterial functionalities and bone cell promotion.

1. Introduction

A wide variety of orthopedic devices are implanted every year in millions of patients suffering from bone-related injuries or diseases, including fracture fixations, artificial joints, and

prostheses [1,2]. The benefits obtained from implants can be numerous, although they are susceptible to multiple problems such as infections, lack of integration, inflammations and total rejection by the host body. Bacterial infections are the main cause of implant failures (ca. 10 %) [1,2]. These are typically caused by adhesion, colonization, and biofilm formation by bacteria colonies on the implant surface after implantation [3]. Bacterial infections require complicated and costly clinical treatments (i.e. up to US\$ 18,000 each) and can lead to morbidity and mortality in patients [4-8]. Therefore, considering the large number of patients requiring orthopedic implants, alternative approaches are urgently needed to prevent implants from bacterial infections. Current therapies to treat bacterial infections are based on prolonged and repetitive systemic administration of therapeutics. Intravenous delivery of antibiotics is the standard treatment, which is usually prescribed for 6-8 weeks upon surgical implantation [9]. However, these therapies are not always effective due to bacterial colonies forming biofilms on the implant surface. These biofilms provide bacteria with protection against the host immune system and also reduce the efficacy of systemic therapy since they act as natural barriers that hinder the diffusion of administered antibiotics [3,10,11].

Therefore, the use of biofilm-disrupting agents and localized administration of antibiotics have become one of the most promising alternatives to address this problem. In this regard, a number of strategies have been developed so far, including bioactive sol-gel glass, injectable polymers, peptides or protein-based surface coatings, poly(methyl methacrylate) (PMMA) beads, and bone cements [12-18]. Nevertheless, these alternatives present some inherent shortcomings, such as toxicity, removal complications due to cemented revisions, exothermic polymerization leading to thermal injury to tissue, protein denaturation that inhibits growth factors, insufficient antibiotics dosage for direct exchange, and low fracture toughness, low mechanical strength and load

bearing capacity [19-23]. In the case of orthopedic implants based on titanium (Ti), one of the most promising approaches to overcome these limitations is to generate a layer of titania nanotubes (TNTs) on the implant surface via electrochemical anodization [24,25]. This electrochemical approach is based on a simple, scalable and cost-effective industrial process that can be applied on currently used medical implants based on Ti and Ti alloys of a variety of forms and shapes (including screws, plates, nails and wires) [26]. TNTs layers have a high surface area and loading capacity, excellent chemical inertness, mechanical robustness, good biocompatibility, tunable nanotube dimensions and surface chemistry. Furthermore, the duration and kinetics of drug released from TNTs structures can be controlled ad-lib by either engineering the nanotubes' dimensions or modifying their surface chemistry, and alternatively, by incorporating polymeric coatings on the TNTs-Ti implant surface through plasma polymerization or dip-coating [27-31]. For these reasons drug-eluting TNTs-Ti implants for localized delivery of therapeutics (e.g. anti-inflammatory, antibiotics, anticancer drugs and proteins) have attracted huge attention during recent years [9,24,25,27-29,31]. However, their potential applicability as an active nanostructured surface for antibacterial proliferation and biofilm formation has not been adequately explored yet. So far, only a few studies have reported on the antibacterial properties of TNTs loaded with antibacterial agents (i.e. antibiotics and silver) [32-38]. Therefore, given the widespread use of Ti-based implants in orthopedics and their susceptibility to clinical complications associated with bacterial biofilms, more in-depth studies should be carried out in order to fully exploit the potential applicability of TNTs in orthopedics. In particular, studies showing combined effect of antibacterial and osteogenic properties of drug-releasing TNTs based Ti implants are scarce. This is a fundamental aspect to translate TNTs-Ti implants into real clinical therapies, where antibacterial properties and bone cell

promotion/integration are recognized as the most critical factors.

Thus, our study is aimed at enhancing the therapeutic performance of drug-releasing TNTs-Ti implants in terms of osteoblast adhesion and antibacterial properties. To this end, we have developed Ti implants featuring two active layers, namely: i) TNTs layer loaded with an antibacterial drug, and ii) a coating based on specific biopolymers with improved osteoblast adhesion and antibacterial properties. This concept is graphically summarized in **Scheme 1**. First, TNTs were synthesized on flat Ti foils by means of electrochemical anodization and loaded with a model antibacterial drug. The top surface of the Ti plates was subsequently coated with a biopolymer film. This coating enables a controlled and extended release of the drug from the nanotubes and, at the same time, improves bone cell adhesion, promotes implant integration, and prevents the formation of bacterial biofilms. Gentamicin sulphate, an aminoglycoside antibiotic commonly prescribed against implant infections, was selected as a model drug due to its wide bactericidal spectrum [39]. To increase their bioavailability and extend their release in a physiological environment, gentamicin molecules were encapsulated in a micelle polymer nanocarrier, namely, d- α -tocopheryl polyethylene glycol 1000 succinate (TPGS) prior to their loading into TNTs. Two bioactive polymers, i.e. polylactic-co-glycolic acid (PLGA) and Chitosan were investigated as functional coatings on gentamicin-loaded TNTs-Ti samples. The osteoblast adhesion and antibacterial properties of the resulting TNTs-Ti samples were assessed through a series of osteoblasts adhesion studies and bacterial bioassays. The adhesion and proliferation of the human osteosarcoma cell line HOS and *Staphylococcus epidermidis* (*S. epidermidis*) on TNTs-Ti samples (i.e. as-produced TNTs-Ti, gentamicin-loaded TNTs-Ti, micelle-encapsulated gentamicin-loaded TNTs-Ti, and PLGA- and Chitosan-coated TNTs-Ti with and without gentamicin loading) and control samples (i.e. tissue culture plastic and bare Ti

metal) were systemically analyzed by optical and electron microscopes.

2. Methods

2.1. Fabrication of TNTs on Ti.

Ti foils (99.6 % titanium with a thickness of 0.25 mm) supplied by Alfa Aesar (USA) were mechanically polished and cleaned by sonication in acetone for 30 min prior to anodization as reported elsewhere [25,26]. After this, TNTs layers were fabricated by anodizing these Ti foils through a two-step electrochemical anodization performed at 100 V in fluoride containing electrolyte (**Supplementary Information – Section 1**). Structural characterization of TNT-Ti samples during the different experimental stages were performed using a field emission scanning electron microscope (FESEM, Quanta 450, FEI).

2.3. Drug and drug-micelle loading in TNTs-Ti samples.

Direct loading of bare gentamicin inside TNTs was performed from an aqueous solution of gentamicin (50 mg/mL) by drop casting the drug solution as described previously [28]. The loading process involved the pipetting of 100 μ L drug solution onto cleaned TNTs-Ti implants nanotube surface and drying the samples in air. After drying, the surface was wiped gently using a soft lint-free tissue to remove any surface bound drug. The process of pipetting, drying and wiping was repeated 20 times to load substantial amount of drugs into the TNTs. For preparing drug encapsulated micelles, *d*- α -tocopheryl polyethylene glycol 1000 succinate (TPGS) polymer, which is a water-miscible, common vitamin E derivative, was used to formulate amphiphilic

micelles as drug carriers for the encapsulation of the model drug. They were synthesized using a simplified lyophilization technique. Firstly, 15 mg micelles were dissolved in 5 mL chloroform. Upon solvent evaporation in a rotary vacuum evaporator under vacuum, a layer of thin organic micellar film was obtained. The micelles were dispersed in 20 mL Milli-Q water, using gentle magnetic stirring for 15 min. The remaining chloroform was removed under reduced pressure via osmosis effect using regenerated cellulose membrane of 15 mm flat width with 20 cm long tubing (Spectrum Labs, Inc.). The loading of drug was performed by adding the aqueous gentamicin into the micelle solution (20 vol. %) under moderate magnetic stirring. Because gentamicin is a water soluble antibiotic, it is highly inferred that the drug exists in the hydrophilic region of TPGS or in the high affinity region of the micelle surface where the drug is retained. Samples were dialyzed against Milli-Q water for two days to eliminate excess drug and obtain the drug-micelle suspension. The same procedure applies for drug-micelle-contained solution, i.e. for the gentamicin-loaded TPGS micelles.

2.4. Coating of drug-loaded TNTs-Ti samples with biopolymers.

Polymer solutions of Chitosan [1 % (w/v) Chitosan + 0.8 % (v/v) acetic acid in Milli-Q water] and poly-(D,L-lactide-co-glycolide) (PLGA) [1 % (w/v) in chloroform] were prepared and each separately coated onto the TNTs-Ti samples by the dip-coating method reported elsewhere [28]. The thickness of the deposited polymer was controlled by the number of dip-coating cycles and was measured by SEM.

2.5. Drug release characterization.

In vitro release of gentamicin from drug-loaded and polymer-coated (PLGA and Chitosan) TNTs-Ti samples was investigated by measuring the changes in UV-visible absorbance with

time (Agilent technologies, Carry 60 spectrophotometer) using a quartz cuvette of 10 mm path length and 1 mL volume (Starna® Pty. Ltd.) (**Supplementary Information – Section 2**).

2.6. Osteoblastic cell culture and analysis.

The osteosarcoma cell line HOS (American Type Culture Collection, Rockville, MD, USA) was used as a model of human osteoblastic cells. This osteosarcoma cell line was chosen due to their similarity with normal osteoblasts in terms of their capability to produce bone matrix [40].

The materials and process for cell culture and TNTs adhesion is described in **Supplementary Information – Section 3**.

2.7. In vitro antibacterial characterization.

Antibacterial bioassays were carried out on TNTs-Ti and PLGA- and Chitosan-coated TNTs-Ti samples, with and without gentamicin payloads. Two gentamicin payloads (*i.e.* bare gentamicin and TPGS-gentamicin micelles) were used to evaluate the antibacterial activity of drug-loaded TNTs-Ti samples. Notice that bare Ti and bare TNTs-Ti samples without drug loading were used as the control samples for comparison. A summary of the performed antibacterial bioassays is presented in **Scheme 2**. Unless otherwise indicated, all aforementioned experiments were repeated in triplicate and statistically treated. Detailed methodology of bacterial incubation and inoculation is provided in **Supplementary Information – Section 4**.

3. Results and discussion

3.1. Structural characterization of TNTs-Ti samples.

SEM analysis was carried out for characterizing the morphology of the prepared TNTs-Ti samples before and after polymer coating, which are presented in **Fig. 1A and B**, respectively. SEM images of the top surface of TNTs-Ti samples (**Fig. 1Ai**) show nanotubes with opened

pores featuring an average diameter of 100 ± 20 nm. The actual size of a TNTs layer fabricated on the surface of Ti plates with a diameter of 10 mm is shown in **Fig. 1Ai** (inset). A high-resolution cross-sectional SEM image of the TNTs is presented in **Fig. 1Aii**, displaying vertically aligned, highly ordered and densely packed arrays of TNTs. Images of the top surface of PLGA- and Chitosan-coated TNTs-Ti samples after dip-coating are presented in **Fig. 1Bi and Bii**, respectively. These images are color-processed to discreetly highlight the ultra-thin film biopolymer coatings on the surface of TNTs-Ti samples. As these images reveal, the textured surface of these polymeric coatings contained micro and nanoscale roughness. However, the surface roughness is much less in comparison to uncoated TNTs. The thickness of the PLGA and Chitosan coatings was estimated to be ~ 2.5 μm and ~ 1.5 μm , respectively, as measured from the SEM images as well as verified by ellipsometry.

3.2. *In vitro* release of gentamicin from TNTs-Ti samples.

Comparative *in vitro* drug release profiles from TNTs-Ti samples loaded with gentamicin and TPGS-gentamicin with and without biopolymer coatings (i.e. PLGA and Chitosan) are provided in **Fig. S1 (Supplementary Information)**. These profiles show a biphasic release pattern composed of an initial fast (burst) phase over the first 6 h and a subsequent slow release phase. The release characteristics obtained from these profiles are listed in **Table 1**, which summarizes the percentage of drug released at specific time intervals (1, 6 and 24 h; and 8, 16, and 26 days) and the total time to complete the drug release. For uncoated TNTs-Ti samples, the release kinetics is divided into two phases, with 77 % of the drug being released in the first 6 h (i.e. initial burst release), followed by a slow release over the following 7 days. Favorable reduction in the burst release and a significant improvement in the overall release periods were observed for TNTs-Ti samples loaded with TPGS-gentamicin micelles. In these TNTs-Ti samples, the

burst release was reduced to 57 % and the elution period extended for up to 10 days.

As for the drug-releasing performance, our results reveal that these biopolymer coatings can extend the release of gentamicin for up to 22 (Chitosan coating) to 26 (PLGA coating) days, in comparison to 7 days provided by gentamicin-loaded TNTs-Ti samples without any biopolymer coating (**Fig. S1, Supplementary Information**). Furthermore, the encapsulation of gentamicin into micelles enabled the extension of drug release and improved released kinetics due to the larger size of the micelle-drug particle, resulting in higher interaction with the nanotubes' walls that eventually led to a delayed release. In addition to this, biopolymer coatings (Chitosan or PLGA) were shown to provide further extension of the release of drug molecules because they are capable of acting as a physical barrier to hinder the direct contact between drugs and the bulk solution. In that regard, the longer release period observed in PLGA-coated TNTs-Ti samples can be related to the thickness of these coatings (2.5 μm) as compared to Chitosan coatings (1.5 μm). The SEM images of biopolymer coated TNT-Ti samples after drug release are provided in **Fig. S2, Supplementary Information** to show the degradation of polymer layer.

3.3. Adhesion and growth of osteoblast on TNTs-Ti samples.

The analyses on the adhesion and proliferation of human osteoblastic cells (HOS) for the five different surfaces (*i.e.* plastic control, bare Ti metal, uncoated TNTs-Ti, Chitosan-coated TNTs-Ti and PLGA-coated TNTs-Ti) are presented in **Fig. 2**. The total number of cells adhered on the surface of these substrates after 1.5 and 24 h was subsequently expressed in percentage, and the results are graphically represented in **Fig. 2A**. Interestingly, the adhesion of HOS osteoblast cells on TNTs-Ti samples was more avid in comparison to the plastic control sample at the early stage (*i.e.* 1.5 h). Moreover, significant differences were observed in the osteoblast-binding properties of TNTs-Ti samples featuring polymeric coatings as well.

For instance, Chitosan-coated TNTs-Ti samples provided the greatest cell attachment during this stage and maintained this trend over the course of the next 24 h. It is worth stressing that the number of HOS cells on plastic and Ti controls increased after 24 h of incubation. HOS cells adhere and proliferate on TNTs and PLGA coatings as well, but relatively poorer performances were found for these surfaces. This analysis revealed that Chitosan-coated TNTs-Ti samples present the best statistical consistency in terms of osteoblast adhesion properties over 24 h of incubation. The ability of the cells to spread on the surface of TNTs-Ti samples was analyzed by cytoskeletal staining and confocal microscopy, presented in **Fig. 2Bi-iv**. Notice that the cellular actin filament networks were observed to be stained with phalloidin (red), whereas the nuclei with DAPI (blue). These images show that osteoblasts were attached and well-spread across the surface of the TNTs-Ti samples, including PLGA- and Chitosan-coated ones, indicating that these polymer coatings are able to support the attachment and viability of osteoblast cells. Chitosan-coated TNTs-Ti samples displayed improved cell adhesion, which can be associated with the positive charge inherently present on Chitosan due to the high density of amino groups. **Fig. 2Bi-iv** show that osteoblasts are well-spread and attached to the surface of polymer-coated TNTs-Ti samples, suggesting that both polymer coatings enhanced osteoblast adhesion and viability. These results are in good coherence with previous studies investigating the ability of Chitosan to promote the formation of bone tissues [42,43]. Note that, the mechanical stability of TNTs grown on Ti substrate is high significance since any delamination or chipping of tubes could lead to severe cytotoxicity at the implant site in the host body. **Figure S3** provides digital photograph of an as-produced TNTs-Ti sample and a TNTs-Ti sample after osteoblast adhesion study, showing no physical damage to TNTs on the surface.

3.4. Antibacterial properties of TNTs-Ti samples.

SEM analysis was employed as the visual assessment method for evaluating the antibacterial properties. **Fig. 3Ai-vii** show SEM images of bacteria on bare Ti and TNTs-Ti samples without drug payload, which were used as control samples. This analysis revealed that the bacterial cells were in healthy conditions featuring typical spherical shape with diameters between 800 nm and 1.1 μm , which fall into the normal size range of a healthy *S. epidermidis*. These bacteria presented a fairly isolated distribution and they appeared in sporadic formation (i.e. in groups of 4-10 cells per colony) on the TNTs-Ti sample surface. No biofilm formation was observed in these samples. Specifically, bacterial cell groups were observed to be random following a circular or linear organization. This behavior was more clearly seen on the surface of TNTs-Ti samples (**Fig. 3Aiii-vii**), as compared with bare Ti (**Fig. 3Ai-ii**). **Fig. 3Aiii** indicates that a greater number of bacterial cells are present on the surface of TNTs samples featuring a layer of TNTs. The bacteria that thrived over the surface of these samples also self-aligned themselves into either linear strands or grape-like micro-colonies (**Fig. 3Aiv-vi**), where they proliferated and were embedded in an ultrathin, slimy matrix of exo-polymeric substances (EPS) secreted by themselves (**Fig. 3Avi**). However, it is inferred that the biofilm was not actually mature as it was still within the motile stage due to the short 1-day assessment, which did not allow sufficient time for its transition to the sessile stage for complete formation. **Fig. 3Avii** shows a SEM image of a single healthy *S. epidermidis* bacterium with a diameter of approximately 800 nm.

SEM images of gentamicin-loaded TNTs-Ti and TPGS- gentamicin-loaded TNTs-Ti samples were compared to evaluate the affinity of *S. epidermidis* to the surface of these samples. Results are presented in **Fig. S4 (Supplementary Information)**. **Fig. S4a and b (Supplementary Information)** confirm a substantial bactericidal effect of gentamicin when it was released from the surface of TNTs-Ti samples. Since the aqueous bacteria suspension was in direct contact

with the drug-loaded TNTs-Ti samples, the potent drug thus created a bactericidal environment as it diffused out from the TNTs-Ti surface to the culture medium. Similar results were obtained with TPGS-gentamicin-loaded TNTs-Ti samples (**Fig. S4c and d, Supplementary Information**). The successful eradication of bacteria from the surface of these TNTs-Ti samples (**Fig. S4c and d, Supplementary Information**) suggests that 24 h is a sufficient contact and exposure time for eliminating bacteria, even though the drug was loaded inside TPGS micelles.

Fig. 3B shows SEM images of TNTs-Ti samples featuring biopolymer coatings of PLGA and Chitosan on their top surface with and without gentamicin payload. Numerous bacteria were detected on the surface of PLGA-coated TNTs-Ti samples, with the whole sample surface covered with bacteria and a thick biofilm, confirming the enhancement of cell adhesion and proliferation over PLGA coatings (**Fig. Bi**). In contrast, large segregated colonies of bacteria were observed on Chitosan-coated TNTs-Ti samples (**Fig. 3Biii**). These visible bacterial cells observed in SEM images were not alive as shown by BacLight™ staining (vide infra) and the viable plate count method (**Fig. S5, Supplementary Information**).

This can be ascribed to the initial stage of contact and adhesion of bacteria on the polymer-modified surface of TNTs-Ti samples and its subsequent death due to the intrinsic antibacterial properties of these biopolymer coatings. Comparing PLGA-coated drug-loaded TNTs-Ti samples with Chitosan-coated counterparts, the former shows a lesser reduction of Gram-positive population (**Fig. 3Bii and iv**, respectively). It is hypothesized that PLGA is capable of inhibiting bacteria growth, although it is unable to impart sufficient cytotoxicity to completely eradicate bacteria on the TNTs-Ti samples. In contrast, Chitosan showed superior performance as a bactericidal agent. A possible reason is the fact that PLGA is more susceptible to degradation through hydrolysis of its ester linkages in an aqueous environment [28]. Another interesting

observation in these tests is that Chitosan exhibits stronger bio-adhesiveness than PLGA, as a vast amount of dead bacterial debris appeared on its surface; this can be assigned to rapid settlement of bacteria due to their negatively charged cell membranes.

In order to confirm the reproducibility of these results and given that the more promising results were obtained with Chitosan-coated gentamicin-loaded TNTs-Ti samples, a set of these TNTs-Ti samples was incubated with bacteria for a longer time period (i.e. 7 days). **Fig. S6a (Supplementary Information)** reveals that bacteria were not able to proliferate properly on the Chitosan-coated gentamicin loaded TNTs-Ti samples. It is inferred that bacteria died as a result of the synergistic combination of two factors: i) the Chitosan coating kept bacteria stagnant and affixed on the surface as small random colonies due to their negatively charged surfaces, which prevented them from forming a protective biofilm, and ii) the bactericidal effect of the released gentamicin, which induced bacterial death. **Fig. S6b (Supplementary Information)** displays magnified images of these samples, elucidating synergistic bactericidal effects between the Chitosan-based coating and biocidal effects of gentamicin. We also observed thinning and decomposition of the Chitosan coatings after long exposure to the liquid medium (i.e. PBS), which is in good agreement with the biodegradability properties of this biopolymer. Furthermore, antibacterial drug release from TNTs-Ti samples plays a crucial role in eradicating bacteria from their surface. It is noteworthy that drug molecules were present in the surrounding environment of the samples as indicated by the *in vitro* drug release profile obtained for Chitosan-coated gentamicin-loaded TNTs-Ti samples **Fig. S1 (Supplementary Information)**. *In vitro* release studies demonstrated the ability of biopolymer coatings to extend the release from 7-10 days to 3 weeks as a function of the thickness of the polymeric coating. It is therefore envisaged that this strategy would protect the inserted samples from bacterial infections during their integration into

the host body.

3.5. *BacLight*TM staining on TNTs-Ti samples.

Bacterial cells on the surface of TNTs-Ti samples were analyzed by the Live/Dead bacterial staining kit *BacLight*TM and the obtained results are displayed in **Fig. 4**. Bright green dots in **Fig. 4Ai and ii** indicate a vast number of live bacteria cells were present on the surface of bare Ti and TNTs-Ti samples, respectively. Both the samples display a thick layer of biofilm produced by the bacterial cells. **Fig. 4Aiii** shows *BacLight*TM staining on a gentamicin-loaded TNTs-Ti sample, confirming that most bacteria were dead and were washed away from the surface. A large number of stained live bacteria (greenish-yellow dots) can be seen on PLGA-coated TNTs-Ti samples (**Fig. 4Bi**). In contrast, a negligible number of such greenish-yellow dots were observed on PLGA-coated TNTs-Ti samples loaded with gentamicin, as shown in **Fig. 4Bii**. This indicates that the release of gentamicin into bacterial medium led to their death, while PLGA prevented their attachment on the sample surface. Chitosan-coated TNTs-Ti samples showed a small amount of greenish-yellow dots on their surface and no dots were observed on Chitosan-coated gentamicin-loaded TNTs-Ti samples as shown in **Fig. 4Biv**. **Fig. 4Bii-iv** show no evidence of biofilm formation, which reveals the antibacterial effect of polymeric coatings on the surface of TNTs-Ti samples as compared to uncoated ones (**Fig. 4Ai-ii and Bi**). Note that the background color observed in these images can be associated with weak adsorption of staining dye molecules on the TNTs-Ti sample surfaces. The antibacterial properties revealed by *BacLight*TM staining are in a good agreement with the results obtained from SEM imaging, revealing that coatings based on Chitosan have a superior bactericidal effect compared with PLGA ones.

3.6. Viable cell count.

Table 2 summarizes the viable cell count for all samples assessed through bacterial testing. A reduction of bacterial counts by a total amount of *ca.* $7.7 \log_{10}$ was substantiated for TNTs-Ti samples. TNTs-Ti samples loaded with gentamicin encapsulated in TPGS, TNTs-Ti samples coated with Chitosan (both with and without gentamicin payload) and PLGA-coated TNTs-Ti loaded with gentamicin displayed complete elimination of bacterial populations from the initial seed value. PLGA-coated TNTs-Ti samples and gentamicin-loaded TNTs-Ti samples recorded quantities of 2.8×10^7 and 4×10^2 bacteria (*i.e.* estimation of 7 and 2 \log_{10} equivalent), which correspond to a reduction of $< 1 \log_{10}$ and $> 5 \log_{10}$, respectively. The antibacterial assay results for the TNTs-Ti samples (except for bare Ti, TNTs and PLGA-TNTs) met the minimum requirement of a 2 \log_{10} reduction from all control inoculums that must be achieved as recommended by the JISZ2801 standard for bactericidal surfaces. Additional information regarding viable cell counts is included in **Fig. S5 (Supplementary Information)**. Therefore, our results confirm the effective antibacterial properties of these biopolymers coatings combined with gentamicin-loaded TNTs-Ti samples.

Chitosan is renowned for its extraordinary antimicrobial properties [46,47]. In our study, we compared antibacterial properties of PLGA- and Chitosan-coated TNTs-Ti samples. We observed that bacterial mortality was seven log values higher for Chitosan-coated TNTs-Ti samples as compared to PLGA-coated ones. PLGA coatings on TNTs-Ti samples (**Fig. 4Bi**) evidence the formation of bacterial biofilms, which was not observed in Chitosan-coated TNTs-Ti samples (**Fig. 4Bi and iii**). Therefore, Chitosan coatings have superior intrinsic antibacterial properties over the PLGA coatings. To further elaborate, a long-term (1 week) antibacterial studies of Chitosan-coated gentamicin-loaded TNTs-Ti samples demonstrated the synergistic

effect of combining biopolymer coatings with antibacterial therapeutics loaded inside TNTs coatings as no bacteria and biofilms were observed in these TNTs-Ti samples (**Fig. S6, Supplementary Information**). The prime reason for antibacterial activity of Chitosan is deemed to the high electrostatic interactions between positively charged amino moieties and the negatively charged bacterial cell membrane leading to chelation of trace metal ions from cell walls and disruption of protein channels and transport of essential nutrients, at pH values above pKa (i.e. neutral pH) [46,47].

In summary, our study has demonstrated that TNTs-Ti samples featuring Chitosan coatings and TPGS-gentamicin payloads can effectively extend the release of therapeutics from TNTs for up to several weeks, thus allowing the promotion of osteoblast cells adhesion and growth without any cytotoxicity and, at the same time, enabling the prevention of bacterial adhesion, proliferation and biofilm formation (**Table S1, Supplementary Information**).

The selective growth of osteoblast cells and eradication of bacteria are dependent on several factors, such as the difference in their structure, size, functionality, mode of contact, location and membrane properties. Therefore, to understand these properties, as well as that of cells, are essential factors to design and engineer orthopedic implants that favor the adhesion and proliferation of osteoblast, while impeding the development of bacterial biofilms. The proposed multi-functional drug-eluting implantable system is envisaged to overcome potential biomedical complications associated with orthopedic implants, as well as be applicable to treat other types of diseases such as bone cancers and osteoporosis.

4. Conclusions

In conclusion, TNTs-Ti substrates were successfully prepared by means of simple electrochemical anodization of Ti foil and were used as a model of multifunctional drug-

releasing bone implant. To endow these TNTs-Ti with osteoblast adhesion and antibacterial properties, TNTs were loaded with TPGS micelles as drug-carrier for the encapsulation of gentamicin drug and coated with a thin layer of biopolymers. These TNTs-Ti surfaces presented a threefold ability: (i) to release gentamicin for extended time periods (*i.e.* up to 3-4 weeks), (ii) excellent osteoblastic adhesion, and (iii) effective antibacterial properties. These results were proven by SEM imaging, BacLight™ staining, and subsequently verified by means of viable cell count. The antibacterial properties of TNTs-Ti samples coated with two biopolymers (*i.e.* PLGA and Chitosan) were evaluated with respect to bare Ti (control), bare TNTs-Ti, TNTs-Ti loaded with gentamicin and TPGS-gentamicin micelles. The results reveal a significant antibacterial effect of Chitosan coatings, which has become more efficient when combined with gentamicin or TPGS-gentamicin payloads inside the TNTs. The reduction of the bacterial viability was well-above the minimum two log value threshold as recommended by the standard for bactericidal surfaces. Hence, our results demonstrate that these remarkable properties of polymer-modified drug-releasing TNTs-Ti samples have equipped them to become potential candidates for future biomedical applications due to their ability to simultaneously deliver therapeutics, reduce implant-related infections and promote osteointegration.

Supporting Information.

The Supporting Information file provides further information about the materials and methods used in this study along with the drug release curves, SEM images of TNTs after drug release, and bacterial viability. This material is available free of charge via the Internet at <http://www.sciencedirect.com>.

Acknowledgments

The authors gratefully acknowledge the financial support provided by the Australian Research Council (ARC) (DP120101680, FT11010071 and DE14010054), The University of South Australia and The University of Adelaide. We would like to thank Dr. Ghafar Servastani from The Hanson Institute for confocal imaging. The contribution of Mr. Saminathan Ramakrishnan, Ms. Renee Ormsby, A/Prof. Gerald Atkins and Prof. David Findlay from the Centre for Orthopaedic & Trauma Research, University of Adelaide, SA, Australia for osteoblast cell study is gratefully acknowledged.

References

- [1] M. Ma, University of British Columbia. Vancouver 2010: Chapter 2.
- [2] D. Davidson, S. Graves, A. Tomkins, J Lynch, R. D. Steiger, R. Vial et al. Hip and Knee Arthroplasty. Aust. Orthop. Assoc. National Joint Replacement Reg. 1 (2013) 181.
- [3] S. Bose, A. K. Ghosh, J.Clin. Diagn. Res. **5** (2011) 127.
- [4] www.privatehealthcareaustralia.org.au/news/stats_and_data/variations-in-care-hip-and-knee-replacement/ Variations in Care Hip and Knee Replacement. Private Healthcare Australia (PHA) assessed 2014, 15 December 2014.
- [5] D. P. Lew, F. A. Waldvogel, The Lancet 364 (2004) 369.
- [6] W. Chen, Y. Liu, H. Courtney, M. Bettenga, C. Agrawal, J. D. Bumgardner, J. L. Ong, *Biomaterials* 27 (2006) 5512.
- [7] T. P. Sculco, Orthopedics 18 (1995) 871.
- [8] R. Trebse, V. Pisot, A. Trampuz, J. Bone Joint Surg., Brit. Vol. 87 (2005) 249.
- [9] M. S. Aw, S. Simovic, J. Addai-Mensah, D. Losic, J. Mater. Chem.21 (2011) 7082.
- [10] J. Costerton, P. S Stewart, E. Greenberg, Science 284 (1999)1318.
- [11] D. Davies, Nat. Rev. Drug Discov. 2 (2003) 114.

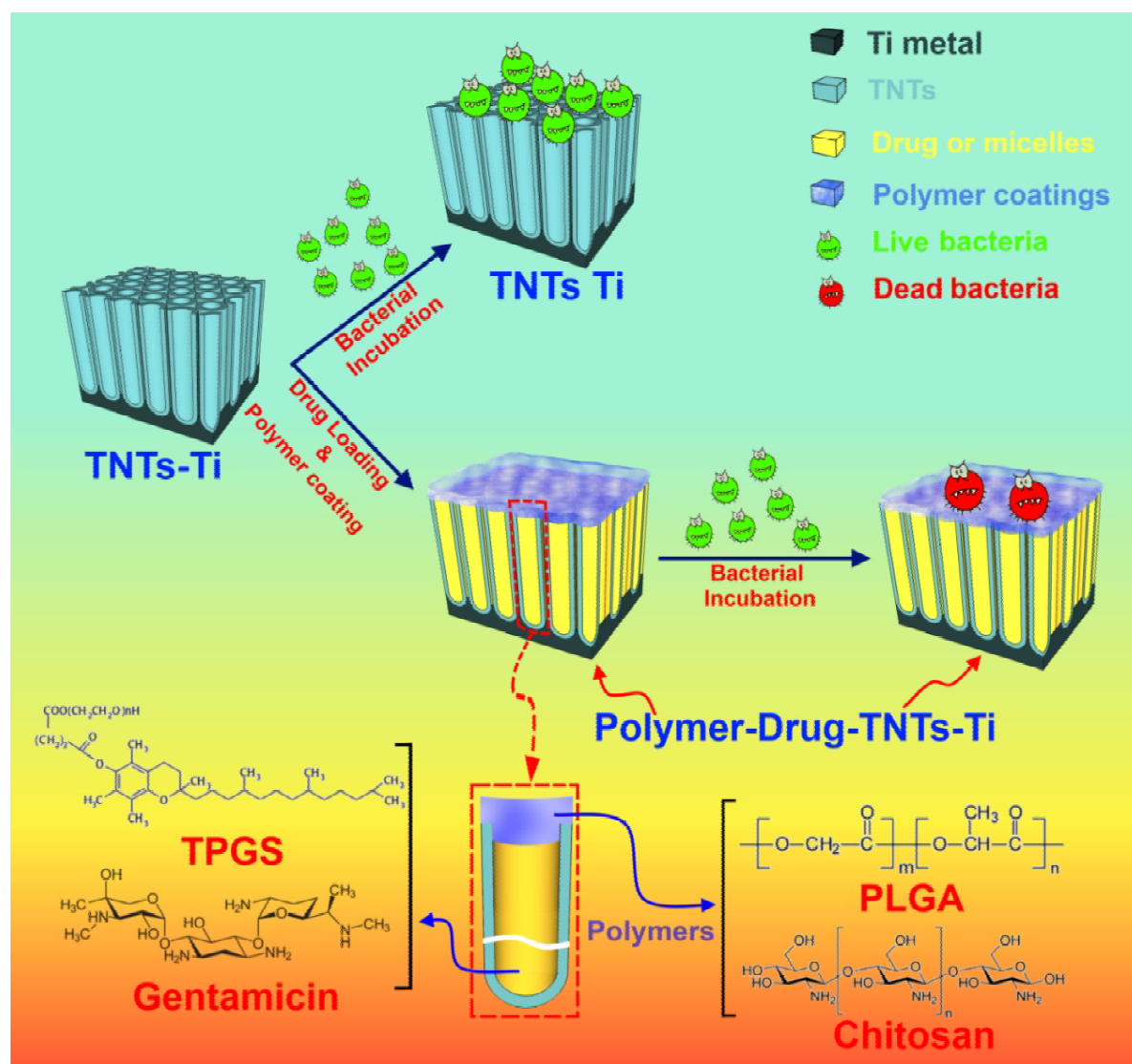
- [12] M. Y. Lan, C. P. Liu, H. H. Huang, S. W. Lee, *PloS one* 8 (2013) e75364.
- [13] A. G. Gristina, *Clin. Microbiol. Newsletter* 16 (1994) 171.
- [14] L. Meseguer-Olmo, M. Ros-Nicolás, M. Clavel-Sainz, V. Vicente-Ortega, M. Alcaraz-Baños, A. Lax-Pérez, D. Arcos, C. V. Ragel, M. Vallet-Regí, *J. Biomed. Mater. Res.* 61 (2002) 458.
- [15] M. Y. Krasko, J. Golenser, A. Nyska, M. Nyska, Y. S. Brin, A. J. Domb, *J. Control. Release* 117 (2007) 90.
- [16] M. Kantlehner, P. Schaffner, D. Finsinger, J. Meyer, A. Jonczyk, B. Diefenbach, B. Nies, G. Hölzemann, S. L. Goodman, H. Kessler, *Chembiochem.* 1 (2000) 107.
- [17] D. Neut, H. van de Belt, I. Stokroos, J. R. van Horn, H. C. van der Mei, H. J. Busscher, *J. Antimicrob. Chemother.* 47 (2001) 885.
- [18] J. Hendriks, J. Van Horn, H. Van Der Mei, H. Busscher, *Biomaterials* 25 (2004) 545.
- [19] P. A. Leggat, U. Kedjarune, *Int. Dent. J.* 53 (2003) 126.
- [20] A. Ricker, P. Liu-Snyder, T. J. Webster, *Int. J. Nanomed.* 3 (2008) 125.
- [21] C. M. Davis, D. J. Berry, W. S. Harmsen, *J. Bone Joint Surg.* 85 (2003) 1264.
- [22] H. Winkler, *Int. J. Med. Sci.* 6 (2009) 247.
- [23] K. Rezwan, Q. Z. Chen, J. J. Blaker, A. R. Boccaccini, *Biomaterials* 27 (2006) 3413.
- [24] D. Losic, S. Simovic, *Expert opin. Drug Delivery* 6 (2009) 1363.
- [25] Q. Huang, Y. Yang, R. Hu, C. Lin, L. Sun, E. A. Vogler, *Colloids and Surfaces B: Biointerfaces* 125 (2015) 134.
- [26] M. Paulose, L. Peng, K. C. Popat, O. K. Varghese, T. J. LaTempa, N. Bao, T. A. Desai, C. A. Grimes, *J. Membr. Sci.* 319 (2008) 199.

- [27] Y. Hu, K. Cai, Z. Luo, D. Xu, D. Xie, Y. Huang, W. Yang, P. Liu, *Acta Biomater.* 8 (2012) 439.
- [28] K. Gulati, S. Ramakrishnan, M. S. Aw, G. J. Atkins, D. M. Findlay, D. Losic, *Acta Biomater.* 8 (2012) 449.
- [29] K. Gulati, M. S. Aw, D. Losic, *D. Int. J. Nanomed.* 7 (2012) 2069.
- [30] X. Chen, K. Cai, J. Fang, M. Lai, Y. Hou, J. Li, Z. Luo, Y. Hu, L. Tang, *Colloids and Surfaces B: Biointerfaces* 103 (2013) 149.
- [31] M. S. Aw, J. Addai-Mensah, D. Losic, *J. Mater. Chem.* 22 (2012) 6561.
- [32] N. Esfandiari A. Simchi, R. Bagheri, *J. Biomed. Mater. Res. Part A* 00A (2013) 1.
- [33] C. Yao, E. B. Slamovich, T. J. Webster, *J. Biomed. Mater. Res. Part A* 85 (2008) 157.
- [34] K. C. Popat, L. Leoni, C. A. Grimes, T. A. Desai, *Biomaterials* 28 (2007) 3188.
- [35] H. Zhang, Y. Sun, A. Tian, X. X. Xue, L. Wang, A. Alquhali, X. Bai, *Int. J. Nanomed.* 8 (2013) 4379.
- [36] L. Zhao, H. Wang, K. Huo, L. Cui, W. Zhang, H. Ni, Y. Zhang, Z. P. K. Chu, *Biomaterials* 32 (2011) 5706.
- [37] K. Huo, X. Zhang, H. Wang, L. Zhao, X. Liu, P. K. Chu, *Biomaterials* 34 (2013) 3467.
- [38] C. Junjian, L. Wang, L. Shi, L. Ren, Y. Wang, *RSC Advances* 4 (2014) 27630.
- [39] R. E. Andersson, G. Lukas, S. Skullman, A. Hugander, *World J. Surg.* 34 (2010) 3042.
- [39] S. B. Rodan, Y. Imai, M. A. Thiede, G. Wesolowski, D. Thompson, Z. Bar-Shavit, S. Shull, K. Mann, G. A. Rodan, *Cancer Res.* 47 (1987) 4961.
- [40] J. A. Waitz, *Methods for dilution antimicrobial susceptibility tests for bacteria that grow aerobically*. Ed. 2009: ed: National Committee for Clinical Laboratory Standards; 1990.
- [41] G. Balasundaram, T. J. Webster, *Macromol. Biosci.* 7 (2007) 635.

- [42] J. D. Bumgardner, R. Wiser, P. D. Gerard, P. Bergin, B. Chestnutt, M. Marini, V. Ramsey, S. H. Elder, J. A. Gilbert, *J. Biomater. Sci, Polymer Ed.* 14 (2003) 423.
- [43] S. H. Uhm, D. H. Song, J. S. Kwon, S. B. Lee, J. G. Han, K. N. Kim, *J. Biomed. Mater. Res. Part B.* 102B (2013) 592.
- [44] A. Taglietti, C. R. Arciola, A. D'Agostino, G. Dacarro, L. Montanaro, D. Campoccia, L. Cucca, M. Vercellino, A. Poggi, P. Pallavicini, L. Visai, *Biomaterials* 35 (2014) 1779.
- [45] M. Kong, X. G. Chen, K. Xing, J. H. Park, *Int. J. Food Microbiol.* 144 (2010) 51.
- [46] H. Tan, Z. Peng, Q. Li, X. Xu, S. Guo, T. Tang, *Biomaterials* 33 (2012) 365.
- [47] S. Y. Ong, J. Wu, S. M. Moochhala, M. H. Tan, J. Lu, *Biomaterials* 29 (2008) 4323.

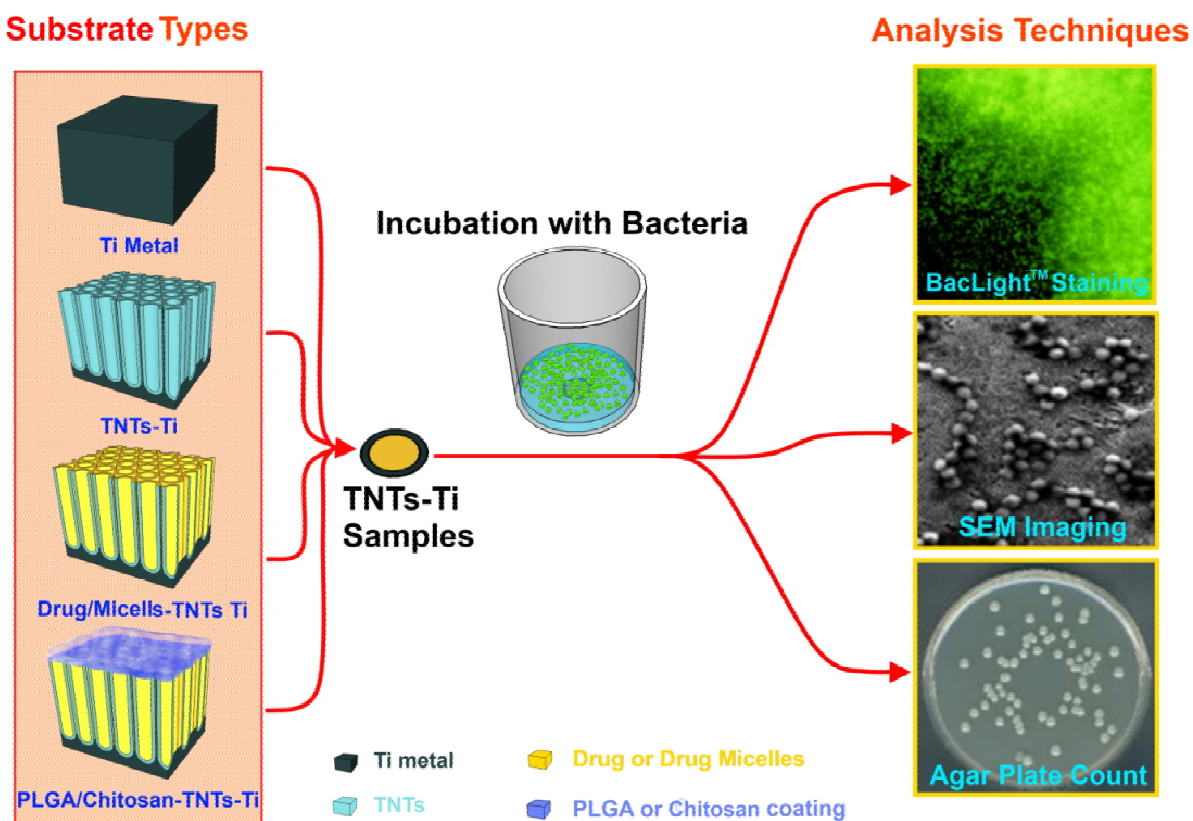
Figures

Scheme 1:



Scheme 1. Schematic diagram summarizing the ability to impart effective antibacterial properties to the proposed TNTs-Ti drug-releasing implants combining drug/micelle (drug/micelle model: Gentamicin/TPGS) payloads and biopolymer coatings (PLGA and Chitosan). The lower part of the scheme shows the chemical structure of the drug/micelle payloads and the two biopolymers used for coating the surface of TNTs-Ti samples. PLGA: polylactic-*co*-glycolic acid.

Scheme 2:



Scheme 2. Flow scheme showing the TNTs-Ti samples employed for antibacterial testing and the characterization techniques used for their qualitative and quantitative analysis. Bacterial growth and biofilm formation on the TNTs-Ti surface were analyzed using BacLight™ staining technique and SEM imaging. Quantitative measurement of surviving bacteria was performed by culturing and counting the viable bacteria.

Figure 1:

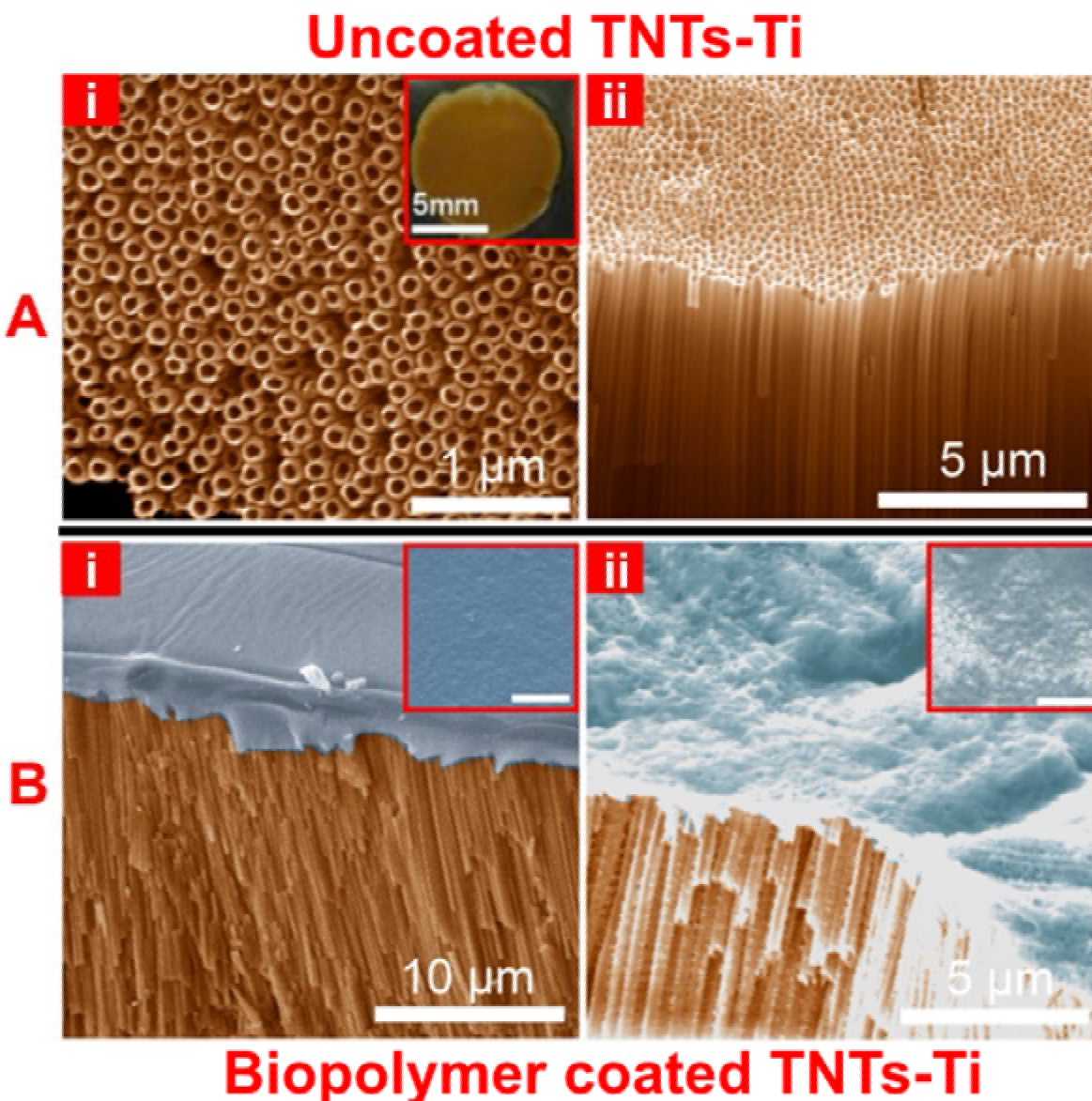


Fig. 1. SEM images of TNTs-Ti fabricated by electrochemical anodization of Ti showing A) uncoated TNTs-Ti substrates with (i) showing the top surface with open nanotubular structure (inset: a digital photograph of the actual TNTs-Ti sample), and (ii) showing an angled cross-sectional image of TNTs with straight and high aspect-ratio nanotubes, B) angled cross-sectional images of TNTs dip-coated with biopolymers (i) PLGA (inset: top-view, Scale bar 1 μm) and (ii) Chitosan (inset: top-view, Scale bar 1 μm).

Figure 2:

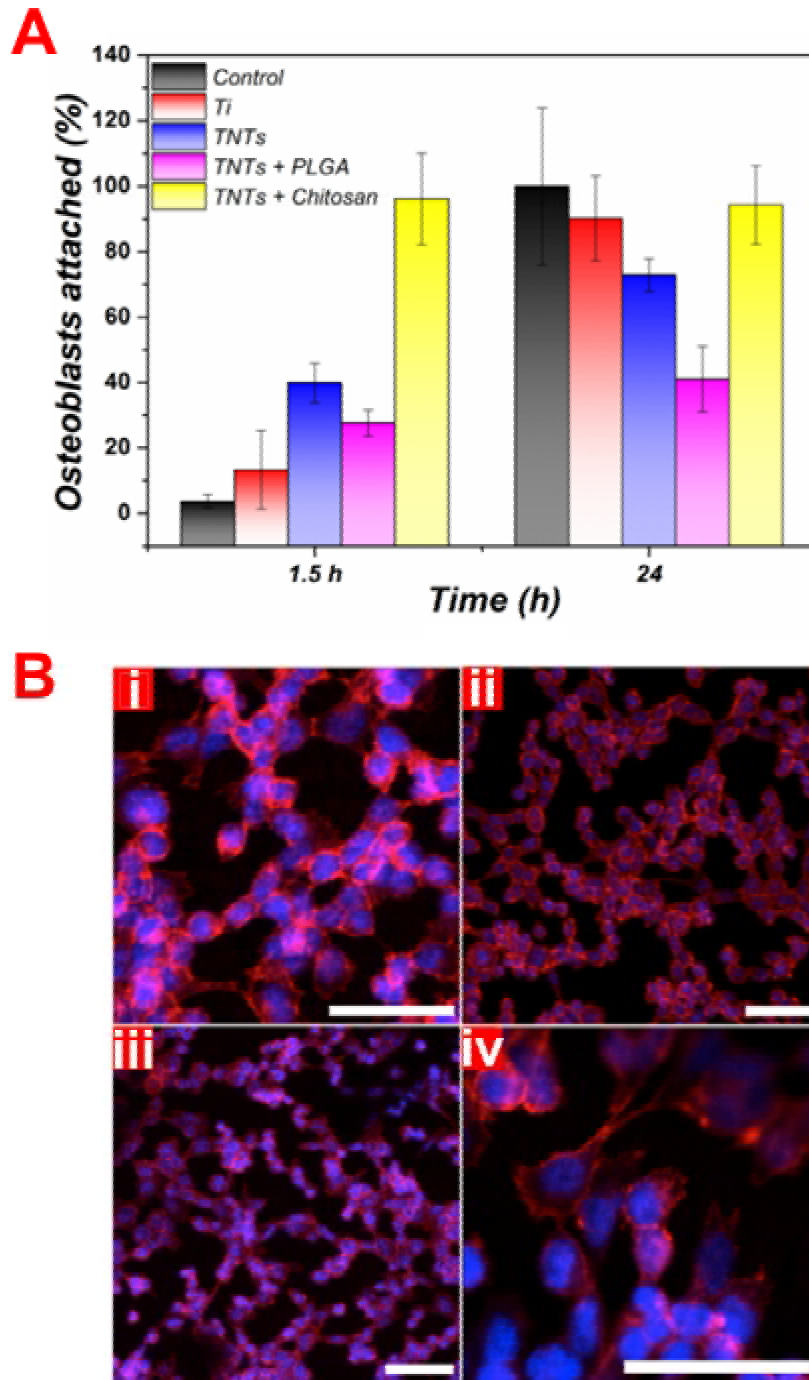


Fig. 2. A) Evaluation of osteoblast adhesion (%) on characterized substrates, including: plastic (control), Ti surface (control), TNTs-Ti, and TNTs-Ti coated with PLGA and Chitosan. Data

shown are means \pm SD from triplicate assays. B) Confocal microscopy images of HOS osteoblast cells on different TNTs-Ti samples (i) Ti metal (control), (ii) TNTs-Ti, (iii) PLGA coated TNTs-Ti, (iv) Chitosan coated TNTs-Ti. Phalloidin (red, cytoskeleton) and DAPI (blue, nuclei) stains show distinct spreading of the attached cells and their morphological outline (Scale bars = 200 μ m).

Figure 3:

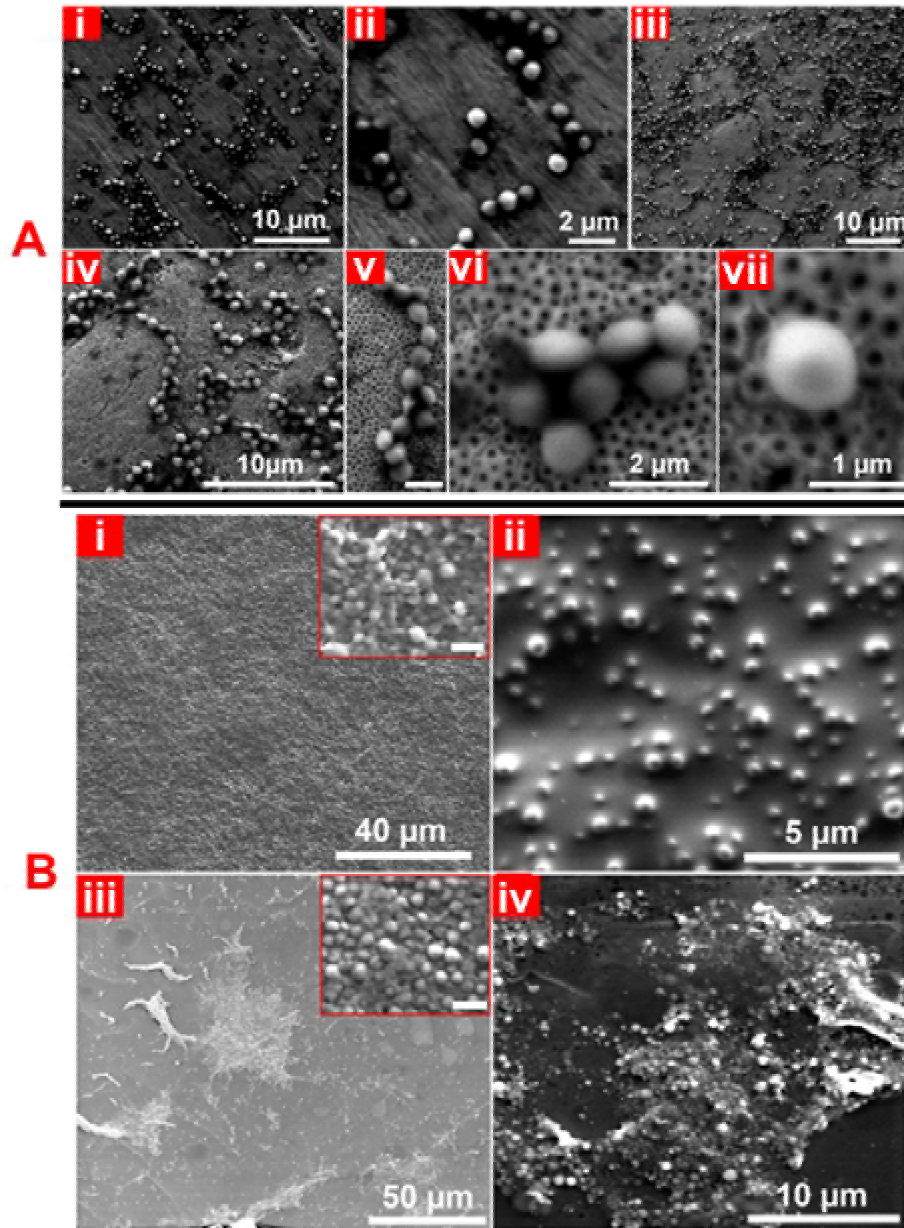


Fig. 3. SEM images of *S. epidermidis* on (A) uncoated Ti and TNTs-Ti substrates (i-ii) Ti metal (control); and (iii-vii) TNTs-Ti implants, showing that the surface is only partially covered by

bacterial colonies, aligned in linear and grape-like cluster configuration (Scale bar for (v): 1 μm). B) SEM images of *S. epidermidis* on TNTs-Ti coated with PLGA (i) without gentamicin (inset: Scale bar 2 μm), and (ii) loaded with gentamicin. SEM images of TNT-Ti coated with Chitosan (iii) without gentamicin (inset: Scale bar 2 μm), and (iv) loaded with gentamicin.

Figure 4:

Accepted Manuscript

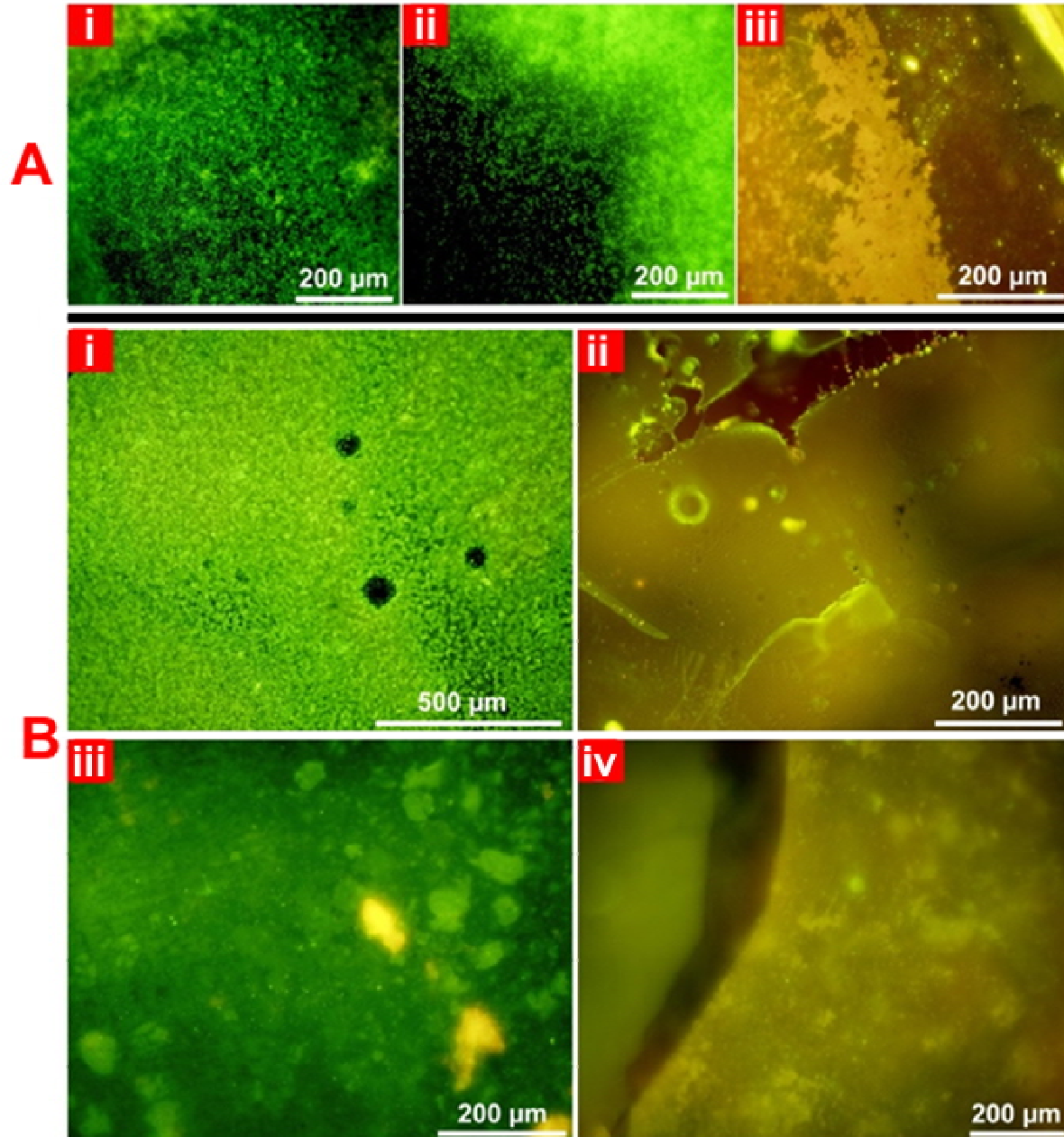


Fig. 4. BacLight™ staining microscopy images of bacterial adherence and biofilm formation on TNTs-Ti samples. A) uncoated Ti metal and TNTs-Ti samples (i) Ti metal (control), (ii) TNTs-Ti, and (iii) Gentamicin-loaded TNTs-Ti. B) PLGA and Chitosan coated TNTs-Ti samples (i) PLGA-coated TNTs-Ti without gentamicin, (ii) PLGA-coated TNTs-Ti loaded with gentamicin, (iii) Chitosan-coated TNTs-Ti without gentamicin, and (iv) Chitosan-coated TNTs-Ti loaded with gentamicin.

Tables

Table 1

Drug release characteristics of prepared TNTs-Ti samples loaded with gentamicin and coated with Chitosan and PLGA polymer films. (Mean \pm SD, n = 3). Here, Gent-TNTs-Ti: gentamicin loaded TNTs-Ti sample, TPGS-Gent-TNTs-Ti: TPGS micelle encapsulated gentamicin loaded TNTs-Ti sample, Chitosan-Gent-TNTs-Ti: gentamicin loaded TNTs-Ti sample coated with Chitosan polymer, and PLGA-Gent-TNTs-Ti: gentamicin loaded TNTs-Ti sample coated with PLGA polymer.

Implant type	Drug release (%)					Total drug elution period (days)
	6 h	1 day	7 days	14 days	21 days	
Gent-TNTs-Ti	77	86	99	100	100	7 \pm 2
TPGS-Gent-TNTs-Ti	57	64	90	100	100	10 \pm 1
Chitosan-Gent-TNTs-Ti	60	66	85	95	99	22 \pm 3
PLGA-Gent-TNTs-Ti	50	55	71	91	98	26 \pm 1

Table 2

Viable bacteria (*S. epidermidis*) counts performed from the overnight bacterial suspension removed from all tested TNTs-Ti samples: Ti metal: titanium metal control, TNTs-Ti: Titania nanotubes grown on Ti metal, PLGA-TNTs-Ti: PLGA coated TNTs-Ti sample, Chitosan-TNTs-Ti: Chitosan coated TNTs-Ti sample, Gent-TNTs-Ti: gentamicin loaded TNTs-Ti sample, TPGS-Gent-TNTs-Ti: TPGS micelle encapsulated gentamicin loaded TNTs-Ti sample, Chitosan-Gent-TNTs-Ti: gentamicin loaded TNTs-Ti sample coated with Chitosan polymer, and PLGA-Gent-TNTs-Ti: gentamicin loaded TNTs-Ti sample coated with PLGA polymer.

Implant type	Viable cell count (CFU/mL)
Ti metal (control)	7.7×10^7
TNTs-Ti	9.5×10^7
PLGA-TNTs-Ti	2.8×10^7
Chitosan- TNTs-Ti	0
Gent-TNTs-Ti	4×10^2
Gent-TPGS-TNTs-Ti	0
PLGA-Gent-TNTs-Ti	0
Chitosan-Gent-TNTs-Ti	0